

FULLY-COUPLED SPHERICAL MODULAR PENDULUM MODEL TO SIMULATE SPACECRAFT PROPELLANT SLOSH

Paolo Cappuccio*, Cody Allard[†] and Hanspeter Schaub[‡]

A spacecraft undergoing general translational and rotational motion can be affected by the sloshing of propellant. A spherical pendulum model is used for simulating this phenomenon because it can better represent the sloshing behavior for rotational dynamics in micro-gravity. This paper develops the fully coupled equations of motion of such a system and presents the solution in a form suitable for the back-substitution method. This modular formulation permits the use of as many pendulums as necessary to approximate the actual sloshing behavior. The general formulation makes minimal assumptions for the rigid portion of the spacecraft and is developed in a frame independent manner making the model applicable to wide range of spacecraft configurations. The model is implemented and verified using energy and momentum conservation in the Basilisk astrodynamics software package. The results of a simulation example of a GPS satellite are shown as an application of the model.

INTRODUCTION

Propellant sloshing can be one of the main disturbances on spacecraft motion. It affects both the on-orbit mission requirements (e.g. attitude control performance, precise pointing, precise orbit determination etc.) and launch requirements. Launch systems have strict requirements on lateral and longitudinal first fundamental spacecraft frequency to avoid dynamic coupling between the low-frequencies of the launch vehicles and the spacecraft modes.¹ The coupling between spacecraft and launcher modes is investigated by many studies. The effect of propellant sloshing is one of the main contributors to this coupling.²

Several studies on the propellant sloshing is based on ground observations³⁻⁵ but the knowledge of sloshing motion in micro-gravity needs still a deep investigation. The most precise way to predict propellant sloshing is to perform computational fluid dynamics (CFD) analysis based on the well-known Navier-Stokes equations.⁶ DNS (direct numerical simulation) provides an accurate prediction of the sloshing but it is expensive in terms of time and computing resources. In particular these computations cannot be executed in real time because a complex CFD simulation could require many days.⁷

In contrast, a simplified model is desirable to analyze the control system performance throughout the whole mission time-line and in a Monte-Carlo environment. Historically two mechanical models have been used to approximate propellant slosh: spring-mass systems and pendulums. The

*Graduate Student, Space and Astronautical Engineering, Sapienza University of Rome.

[†]Graduate Student, Aerospace Engineering Sciences, University of Colorado Boulder.

[‡]Professor, Glenn L. Murphy Chair, Department of Aerospace Engineering Sciences, University of Colorado, 431 UCB, Colorado Center for Astrodynamics Research, Boulder, CO 80309-0431. AAS Fellow.

spring-mass system provides a good approximation in a gravity field or during a strong acceleration phase.² On the other hand, in micro-gravity the pendulum model is preferred.⁸ Additionally, pendulum models can better approximate the sloshing phenomenon in a micro-gravity environment when the spacecraft is undergoing attitude maneuvers.⁹ These models, when used simultaneously, can better approximate the overall sloshing phenomenon from a translational and attitude dynamics perspective.⁹

This paper develops a fully-coupled dynamics model for propellant slosh modeled as spherical pendulums using Newtonian/Eulerian mechanics. The model is developed from first-principles, therefore, conservation of energy and momentum can be verified. In contrast to earlier work, the equations of motion are developed in a manner suitable for the recently developed back-substitution method for complex spacecraft dynamics.¹⁰ The spacecraft relative flexing, or sloshing in this case, is written in a manner where their contributions to the rigid spacecraft hub components is analytically decoupled. This form allows the complex spacecraft equations of motion to be elegantly numerically implemented in a modular fashion. For example, if in addition to fuel slosh the spacecraft is also subject to an imbalanced reaction wheel,¹¹ or a flexible panel,¹² the fuel slosh equations do not need to be re-derived even though all these modes are coupled. Rather, the back-substitution form allows such dynamic effectors to be added individually and still retain the full nonlinear coupling.

The first section presents a general outline of the reference systems and reference points necessary to derive the equation of motions, obtained in the second section. In the third section, the back substitution method¹⁰ is derived to obtain better computational efficiency. In the fourth section, the equation of energy and momentum conservation are derived and in the fifth section a method to avoid singularities due to the reference frame definitions is derived. Finally, in the last section an example of the implementation of this model is presented and it is verified through energy and momentum conservation.

PROBLEM STATEMENT

The spacecraft model considered in this work is composed by a rigid hub, a propellant tank and N_P lumped masses simulating the propellant. The Basilisk software package* allows for multiple phenomena at the same time (e.g. solar panel rotations, maneuvers, reaction wheels operations etc.), thanks to the versatile structure of this software.¹⁰ Subscript j indicates the j^{th} propellant slosh mass, m_j . Figure 1 shows reference frame and key point definitions used for this formulation.

Four coordinate frames are defined for this formulation. The inertial reference frame is indicated by $\mathcal{N} : \{\hat{n}_1, \hat{n}_2, \hat{n}_3\}$. The body fixed coordinate frame, $\mathcal{B} : \{\hat{b}_1, \hat{b}_2, \hat{b}_3\}$, which is fixed with respect to the hub and can be oriented in any direction. Point B indicates the origin of the body fixed reference frame, which can be any point fixed with respect to the hub. The initial pendulum frame, $\mathcal{P}_{0,j} : \{\hat{p}_{0,j,1}, \hat{p}_{0,j,2}, \hat{p}_{0,j,3}\}$, is a frame with its origin located at the tank geometrical center, T . The $\mathcal{P}_{0,j}$ frame is a fixed frame with respect to the body frame, oriented such that $\hat{p}_{0,j,1}$ points to the propellant slosh mass in its initial position, P_j . The constant distance from point T to point P_j is defined as l_j , while with \mathbf{l}_j is indicated the vector from T to $P_{c,j}$, the instantaneous position of the propellant slosh mass m_j . B_c is the location of the center of mass of the rigid hub and \mathbf{d} is vector from the center of the body reference system to the tank geometrical center.

Figure 2 provides further detail of the propellant slosh parameters and reference frames. As seen

*<http://hanspeterschaub.info/bskMain.html>

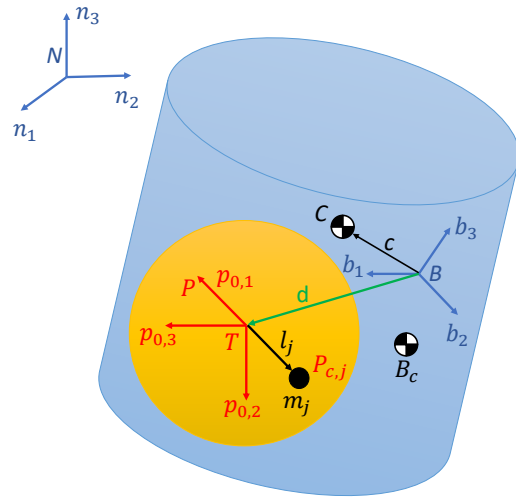


Figure 1: Frame and variable definitions used for formulation

in Figure 1, an individual slosh particle is free to move in every direction constrained to a sphere while connected by rigid weightless rod to the geometrical center of the tank. A linear damper effect is considered using a damping matrix, D . The variables, φ_j and ϑ_j are state variables and quantify the angular displacement from initial position for the corresponding slosh mass.

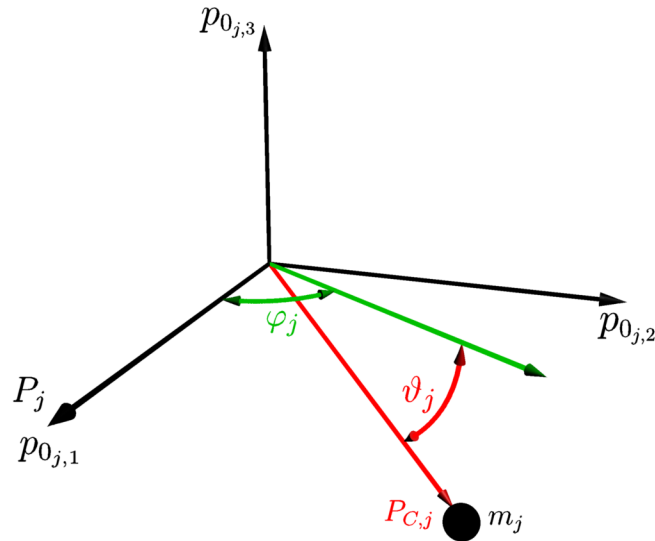


Figure 2: Further detail of propellant slosh and reference frames

DERIVATION OF EQUATIONS OF MOTION

Rigid Spacecraft Bus Translational Motion

Regarding the derivation of the equations of motion (EOMs), the same back-substitution approach used in others Basilisk package's modules is considered in this work; such as hinged solar panels

dynamics,¹³ spring-mass propellant slosh model¹² and reaction wheel dynamics.¹¹ The derivation begins with Newton's first law¹⁴ for the center of mass of the spacecraft:

$$\ddot{\mathbf{r}}_{C/N} = \frac{\mathbf{F}}{m_{sc}} \quad (1)$$

Ultimately, the acceleration of the body frame or point B is desired:

$$\ddot{\mathbf{r}}_{B/N} = \ddot{\mathbf{r}}_{C/N} - \ddot{\mathbf{c}} \quad (2)$$

The definition of \mathbf{c} can be seen in Eq. (3):

$$\mathbf{c} = \frac{1}{m_{sc}} \left(m_{bus} \mathbf{r}_{B_c/B} + \sum_{j=1}^{N_P} m_j \mathbf{r}_{P_{c,j}/B} \right) \quad (3)$$

The time derivative of \mathbf{c} with respect to the body frame is needed to compute the inertial time derivative of \mathbf{c} . A time derivative of any vector, \mathbf{v} , with respect to the body frame is denoted by \mathbf{v}' ; the inertial time derivative is indicated as $\dot{\mathbf{v}}$. The first and second body-relative time derivatives of \mathbf{c} are seen in:

$$\mathbf{c}' = \frac{1}{m_{sc}} \left(\sum_{j=1}^{N_P} m_j \mathbf{r}'_{P_{c,j}/B} \right) \quad (4)$$

$$\mathbf{c}'' = \frac{1}{m_{sc}} \left(\sum_{j=1}^{N_P} m_j \mathbf{r}''_{P_{c,j}/B} \right) \quad (5)$$

Remembering that the derivative of \mathbf{d} is null respect to the body frame, the first and second body time derivatives of $\mathbf{r}_{P_{c,j}/B}$ are:

$$\mathbf{r}_{P_{c,j}/B} = l_j \begin{bmatrix} \cos(\varphi_j) \cos(\vartheta_j) \\ \sin(\varphi_j) \cos(\vartheta_j) \\ -\sin(\vartheta_j) \end{bmatrix} + \mathbf{d} \quad (6)$$

$$\mathbf{r}'_{P_{c,j}/B} = l_j \begin{bmatrix} -\dot{\varphi}_j \sin(\varphi_j) \cos(\vartheta_j) - \dot{\vartheta}_j \cos(\varphi_j) \sin(\vartheta_j) \\ \dot{\varphi}_j \cos(\varphi_j) \cos(\vartheta_j) - \dot{\vartheta}_j \sin(\varphi_j) \sin(\vartheta_j) \\ -\dot{\vartheta}_j \cos(\vartheta_j) \end{bmatrix} \quad (7)$$

$$\mathbf{r}''_{P_{c,j}/B} = l_j \begin{bmatrix} -\ddot{\varphi}_j \sin(\varphi_j) \cos(\vartheta_j) - \ddot{\vartheta}_j \cos(\varphi_j) \sin(\vartheta_j) - \dot{\varphi}_j^2 \cos(\varphi_j) \cos(\vartheta_j) \\ -\dot{\vartheta}_j^2 \cos(\varphi_j) \cos(\vartheta_j) + 2\dot{\varphi}_j \dot{\vartheta}_j \sin(\varphi_j) \sin(\vartheta_j) \\ \ddot{\varphi}_j \cos(\varphi_j) \cos(\vartheta_j) - \ddot{\vartheta}_j \sin(\varphi_j) \sin(\vartheta_j) - \dot{\varphi}_j^2 \sin(\varphi_j) \cos(\vartheta_j) \\ -\dot{\vartheta}_j^2 \sin(\varphi_j) \cos(\vartheta_j) - 2\dot{\varphi}_j \dot{\vartheta}_j \cos(\varphi_j) \sin(\vartheta_j) \\ -\ddot{\vartheta}_j \cos(\vartheta_j) + \dot{\vartheta}_j^2 \sin(\vartheta_j) \end{bmatrix} \quad (8)$$

Eqs. (4) and (5) are next reformulated to include these new definitions:

$$\mathbf{c}' = \frac{1}{m_{sc}} \sum_{j=1}^{N_P} m_j l_j \left[\left(-\dot{\varphi}_j \sin(\varphi_j) \cos(\vartheta_j) - \dot{\vartheta}_j \cos(\varphi_j) \sin(\vartheta_j) \right) \hat{\mathbf{p}}_{0,j,1} + \left(\dot{\varphi}_j \cos(\varphi_j) \cos(\vartheta_j) - \dot{\vartheta}_j \sin(\varphi_j) \sin(\vartheta_j) \right) \hat{\mathbf{p}}_{0,j,2} - \dot{\vartheta}_j \cos(\vartheta_j) \hat{\mathbf{p}}_{0,j,3} \right] \quad (9)$$

$$\begin{aligned}
\mathbf{c}'' = & \frac{1}{m_{sc}} \sum_{j=1}^{N_P} m_j l_j \left[\left(-\ddot{\varphi}_j \sin(\varphi_j) \cos(\vartheta_j) - \ddot{\vartheta}_j \cos(\varphi_j) \sin(\vartheta_j) - \dot{\varphi}_j^2 \cos(\varphi_j) \cos(\vartheta_j) - \dot{\vartheta}_j^2 \cos(\varphi_j) \cos(\vartheta_j) \right. \right. \\
& + 2\dot{\varphi}_j \dot{\vartheta}_j \sin(\varphi_j) \sin(\vartheta_j) \left. \right) \hat{\mathbf{p}}_{0,j,1} + \left(\ddot{\varphi}_j \cos(\varphi_j) \cos(\vartheta_j) - \ddot{\vartheta}_j \sin(\varphi_j) \sin(\vartheta_j) - \dot{\varphi}_j^2 \sin(\varphi_j) \cos(\vartheta_j) \right. \\
& \left. \left. - \dot{\vartheta}_j^2 \sin(\varphi_j) \cos(\vartheta_j) - 2\dot{\varphi}_j \dot{\vartheta}_j \cos(\varphi_j) \sin(\vartheta_j) \right) \hat{\mathbf{p}}_{0,j,2} + \left(-\ddot{\vartheta}_j \cos(\vartheta_j) + \dot{\vartheta}_j^2 \sin(\vartheta_j) \right) \hat{\mathbf{p}}_{0,j,3} \right] \quad (10)
\end{aligned}$$

Using the transport theorem¹⁴ yields the following definition for $\ddot{\mathbf{c}}$:

$$\ddot{\mathbf{c}} = \mathbf{c}'' + 2\boldsymbol{\omega}_{B/N} \times \mathbf{c}' + \dot{\boldsymbol{\omega}}_{B/N} \times \mathbf{c} + \boldsymbol{\omega}_{B/N} \times (\boldsymbol{\omega}_{B/N} \times \mathbf{c}) \quad (11)$$

Eq. (2) is updated to include Eq. (11):

$$\ddot{\mathbf{r}}_{B/N} = \ddot{\mathbf{r}}_{C/N} - \mathbf{c}'' - 2\boldsymbol{\omega}_{B/N} \times \mathbf{c}' - \dot{\boldsymbol{\omega}}_{B/N} \times \mathbf{c} - \boldsymbol{\omega}_{B/N} \times (\boldsymbol{\omega}_{B/N} \times \mathbf{c}) \quad (12)$$

Substituting Eq.(10) into Eq.(12) results in:

$$\begin{aligned}
\ddot{\mathbf{r}}_{B/N} = & \ddot{\mathbf{r}}_{C/N} - \frac{1}{m_{sc}} \sum_{j=1}^{N_P} m_j l_j \left[\left(-\ddot{\varphi}_j \sin(\varphi_j) \cos(\vartheta_j) - \ddot{\vartheta}_j \cos(\varphi_j) \sin(\vartheta_j) - \dot{\varphi}_j^2 \cos(\varphi_j) \cos(\vartheta_j) \right. \right. \\
& - \dot{\vartheta}_j^2 \cos(\varphi_j) \cos(\vartheta_j) + 2\dot{\varphi}_j \dot{\vartheta}_j \sin(\varphi_j) \sin(\vartheta_j) \left. \right) \hat{\mathbf{p}}_{0,j,1} + \left(\ddot{\varphi}_j \cos(\varphi_j) \cos(\vartheta_j) - \ddot{\vartheta}_j \sin(\varphi_j) \sin(\vartheta_j) \right. \\
& \left. - \dot{\varphi}_j^2 \sin(\varphi_j) \cos(\vartheta_j) - \dot{\vartheta}_j^2 \sin(\varphi_j) \cos(\vartheta_j) - 2\dot{\varphi}_j \dot{\vartheta}_j \cos(\varphi_j) \sin(\vartheta_j) \right) \hat{\mathbf{p}}_{0,j,2} + \left(-\ddot{\vartheta}_j \cos(\vartheta_j) \right. \\
& \left. + \dot{\vartheta}_j^2 \sin(\vartheta_j) \right) \hat{\mathbf{p}}_{0,j,3} \left. \right] - 2\boldsymbol{\omega}_{B/N} \times \mathbf{c}' - \dot{\boldsymbol{\omega}}_{B/N} \times \mathbf{c} - \boldsymbol{\omega}_{B/N} \times (\boldsymbol{\omega}_{B/N} \times \mathbf{c}) \quad (13)
\end{aligned}$$

Moving second order terms to the left hand side, introducing the tilde matrix, to replace the cross product operators, and rearranging the terms, Eq. (13) simplifies to:

$$\begin{aligned}
\ddot{\mathbf{r}}_{B/N} - [\tilde{\mathbf{c}}] \dot{\boldsymbol{\omega}}_{B/N} - \frac{1}{m_{sc}} \sum_{j=1}^{N_P} m_j l_j \left[\left(\sin(\varphi_j) \cos(\vartheta_j) \hat{\mathbf{p}}_{0,j,1} - \cos(\varphi_j) \cos(\vartheta_j) \hat{\mathbf{p}}_{0,j,2} \right) \ddot{\varphi}_j \right. \\
+ \left(\cos(\varphi_j) \sin(\vartheta_j) \hat{\mathbf{p}}_{0,j,1} + \sin(\varphi_j) \sin(\vartheta_j) \hat{\mathbf{p}}_{0,j,2} + \cos(\vartheta_j) \hat{\mathbf{p}}_{0,j,3} \right) \ddot{\vartheta}_j \left. \right] = \ddot{\mathbf{r}}_{C/N} - 2[\tilde{\boldsymbol{\omega}}_{B/N}] \mathbf{c}' \\
- [\tilde{\boldsymbol{\omega}}_{B/N}] [\tilde{\boldsymbol{\omega}}_{B/N}] \mathbf{c} - \frac{1}{m_{sc}} \sum_{j=1}^{N_P} m_j l_j \left[\left(-\cos(\varphi_j) \cos(\vartheta_j) \hat{\mathbf{p}}_{0,j,1} - \sin(\varphi_j) \cos(\vartheta_j) \hat{\mathbf{p}}_{0,j,2} \right) \dot{\varphi}_j^2 \right. \\
+ \left(-\cos(\varphi_j) \cos(\vartheta_j) \hat{\mathbf{p}}_{0,j,1} - \sin(\varphi_j) \cos(\vartheta_j) \hat{\mathbf{p}}_{0,j,2} + \sin(\vartheta_j) \hat{\mathbf{p}}_{0,j,3} \right) \dot{\vartheta}_j^2 \\
\left. + \left(2 \sin(\varphi_j) \sin(\vartheta_j) \hat{\mathbf{p}}_{0,j,1} - 2 \cos(\varphi_j) \sin(\vartheta_j) \hat{\mathbf{p}}_{0,j,2} \right) \dot{\varphi}_j \dot{\vartheta}_j \right] \quad (14)
\end{aligned}$$

Equation (14) is the translational motion equation and is the first EOM needed to describe the motion of the spacecraft. The following section develops the second EOM needed in the derivation of the method.

Rigid Spacecraft Bus Rotational Motion

To obtain the spacecraft rotational equation of motion, the Euler's equation¹⁴ is used. When the body fixed coordinate frame origin is not coincident with the center of mass of the body, the modified Euler's equation is:

$$\dot{\mathbf{H}}_{sc,B} = \mathbf{L}_B + m_{sc}\ddot{\mathbf{r}}_{B/N} \times \mathbf{c} \quad (15)$$

where \mathbf{L}_B is the total external torque about point B . The definition of the angular momentum vector of the spacecraft about point B is:

$$\mathbf{H}_{sc,B} = [I_{bus,B_c}]\boldsymbol{\omega}_{B/N} + m_{bus}\mathbf{r}_{B_c/B} \times \dot{\mathbf{r}}_{B_c/B} + \sum_{j=1}^{N_P} m_j \mathbf{r}_{P_{c,j}/B} \times \dot{\mathbf{r}}_{P_{c,j}/B} \quad (16)$$

Now the inertial time derivative of Eq. (16) is taken and yields:

$$\begin{aligned} \dot{\mathbf{H}}_{sc,B} = [I_{bus,B_c}]\dot{\boldsymbol{\omega}}_{B/N} + \boldsymbol{\omega}_{B/N} \times [I_{bus,B_c}]\boldsymbol{\omega}_{B/N} + m_{bus}\mathbf{r}_{B_c/B} \times \ddot{\mathbf{r}}_{B_c/B} \\ + \sum_{j=1}^{N_P} m_j \mathbf{r}_{P_{c,j}/B} \times \ddot{\mathbf{r}}_{P_{c,j}/B} \end{aligned} \quad (17)$$

The terms $\ddot{\mathbf{r}}_{B_c/B}$ and $\ddot{\mathbf{r}}_{P_{c,j}/B}$ are found using the transport theorem, and knowing that $\mathbf{r}_{B_c/B}$ is fixed with respect to the body frame, the body frame relative derivatives are zero.

$$\ddot{\mathbf{r}}_{B_c/B} = \dot{\boldsymbol{\omega}}_{B/N} \times \mathbf{r}_{B_c/B} + \boldsymbol{\omega}_{B/N} \times (\boldsymbol{\omega}_{B/N} \times \mathbf{r}_{B_c/B}) \quad (18)$$

$$\ddot{\mathbf{r}}_{P_{c,j}/B} = \mathbf{r}''_{P_{c,j}/B} + 2\boldsymbol{\omega}_{B/N} \times \mathbf{r}'_{P_{c,j}/B} + \dot{\boldsymbol{\omega}}_{B/N} \times \mathbf{r}_{P_{c,j}/B} + \boldsymbol{\omega}_{B/N} \times (\boldsymbol{\omega}_{B/N} \times \mathbf{r}_{P_{c,j}/B}) \quad (19)$$

Incorporating Eqs. (18) and (19) into Eq. (17), applying the Jacobi identity,¹⁵ $(\mathbf{a} \times \mathbf{b}) \times \mathbf{c} = \mathbf{a} \times (\mathbf{b} \times \mathbf{c}) - \mathbf{b} \times (\mathbf{a} \times \mathbf{c})$, to the cross products and rearranging the terms, Eq. (19) results in:

$$\begin{aligned} \dot{\mathbf{H}}_{sc,B} = & \left\{ [I_{bus,B_c}] + m_{bus}[\tilde{\mathbf{r}}_{B_c/B}][\tilde{\mathbf{r}}_{B_c/B}]^T + \sum_{j=1}^{N_P} m_j [\tilde{\mathbf{r}}_{P_{c,j}/B}][\tilde{\mathbf{r}}_{P_{c,j}/B}]^T \right\} \dot{\boldsymbol{\omega}}_{B/N} \\ & + \boldsymbol{\omega}_{B/N} \times \left\{ [I_{bus,B_c}] + m_{bus}[\tilde{\mathbf{r}}_{B_c/B}][\tilde{\mathbf{r}}_{B_c/B}]^T + \sum_{j=1}^{N_P} m_j [\tilde{\mathbf{r}}_{P_{c,j}/B}][\tilde{\mathbf{r}}_{P_{c,j}/B}]^T \right\} \boldsymbol{\omega}_{B/N} \\ & + \sum_{j=1}^{N_P} m_j \left\{ \mathbf{r}_{P_{c,j}/B} \times \mathbf{r}''_{P_{c,j}/B} - \left[[\tilde{\mathbf{r}}_{P_{c,j}/B}][\tilde{\mathbf{r}}'_{P_{c,j}/B}] + [\tilde{\mathbf{r}}'_{P_{c,j}/B}][\tilde{\mathbf{r}}_{P_{c,j}/B}] \right] \boldsymbol{\omega}_{B/N} \right. \\ & \left. + \boldsymbol{\omega}_{B/N} \times (\mathbf{r}_{P_{c,j}/B} \times \mathbf{r}'_{P_{c,j}/B}) \right\} \end{aligned} \quad (20)$$

Applying the parallel axis theorem the following inertia tensor terms are defined as:

$$[I_{bus,B}] = [I_{bus,B_c}] + m_{bus}[\tilde{\mathbf{r}}_{B_c/B}][\tilde{\mathbf{r}}_{B_c/B}]^T \quad (21)$$

$$[I_{sc,B}] = [I_{bus,B}] + \sum_{j=1}^{N_P} m_j [\tilde{\mathbf{r}}_{P_{c,j}/B}][\tilde{\mathbf{r}}_{P_{c,j}/B}]^T \quad (22)$$

Taking the body-relative time derivative of Equation (22) yields:

$$[I'_{sc,B}] = - \sum_{j=1}^{N_P} m_j \left([\tilde{\mathbf{r}}'_{P_{c,j}/B}] [\tilde{\mathbf{r}}_{P_{c,j}/B}] + [\tilde{\mathbf{r}}_{P_{c,j}/B}] [\tilde{\mathbf{r}}'_{P_{c,j}/B}] \right) \quad (23)$$

Using Eqs. (22) and (23) to simplify results in Eq. (20), the following simplified equation is obtained:

$$\begin{aligned} \dot{\mathbf{H}}_{sc,B} = [I_{sc,B}] \dot{\boldsymbol{\omega}}_{B/N} + \boldsymbol{\omega}_{B/N} \times [I_{sc,B}] \boldsymbol{\omega}_{B/N} + [I'_{sc,B}] \boldsymbol{\omega}_{B/N} + \sum_{j=1}^{N_P} \left[m_j \mathbf{r}_{P_{c,j}/B} \times \mathbf{r}''_{P_{c,j}/B} \right. \\ \left. + m_j \boldsymbol{\omega}_{B/N} \times \left(\mathbf{r}_{P_{c,j}/B} \times \mathbf{r}'_{P_{c,j}/B} \right) \right] \quad (24) \end{aligned}$$

Eqs. (15) and (24) are equated and yield:

$$\begin{aligned} \mathbf{L}_B + m_{sc} \ddot{\mathbf{r}}_{B/N} \times \mathbf{c} = [I_{sc,B}] \dot{\boldsymbol{\omega}}_{B/N} + \boldsymbol{\omega}_{B/N} \times [I_{sc,B}] \boldsymbol{\omega}_{B/N} + [I'_{sc,B}] \boldsymbol{\omega}_{B/N} + \sum_{j=1}^{N_P} \left[m_j \mathbf{r}_{P_{c,j}/B} \times \mathbf{r}''_{P_{c,j}/B} \right. \\ \left. + m_j \boldsymbol{\omega}_{B/N} \times \left(\mathbf{r}_{P_{c,j}/B} \times \mathbf{r}'_{P_{c,j}/B} \right) \right] \quad (25) \end{aligned}$$

Finally, using tilde matrix and simplifying the modified Euler equation, which is the second EOM necessary to describe the motion of the spacecraft, is obtained. Rearranging Eq. (25) to be in the same form as the previous sections results in:

$$\begin{aligned} m_{sc} [\tilde{\mathbf{c}}] \ddot{\mathbf{r}}_{B/N} + [I_{sc,B}] \dot{\boldsymbol{\omega}}_{B/N} - \sum_{j=1}^{N_P} m_j l_j [\tilde{\mathbf{r}}_{P_{c,j}/B}] \left[\left(\sin(\varphi_j) \cos(\vartheta_j) \hat{\mathbf{p}}_{0,j,1} - \cos(\varphi_j) \cos(\vartheta_j) \hat{\mathbf{p}}_{0,j,2} \right) \ddot{\varphi}_j + \right. \\ \left. + \left(\cos(\varphi_j) \sin(\vartheta_j) \hat{\mathbf{p}}_{0,j,1} + \sin(\varphi_j) \sin(\vartheta_j) \hat{\mathbf{p}}_{0,j,2} + \cos(\vartheta_j) \hat{\mathbf{p}}_{0,j,3} \right) \ddot{\vartheta}_j \right] = \mathbf{L}_B - [\tilde{\boldsymbol{\omega}}_{B/N}] [I_{sc,B}] \boldsymbol{\omega}_{B/N} + \\ - [I'_{sc,B}] \boldsymbol{\omega}_{B/N} - \sum_{j=1}^{N_P} m_j \left\{ [\tilde{\boldsymbol{\omega}}_{B/N}] [\tilde{\mathbf{r}}_{P_{c,j}/B}] \mathbf{r}'_{P_{c,j}/B} + l_j [\tilde{\mathbf{r}}_{P_{c,j}/B}] \left[\left(-\cos(\varphi_j) \cos(\vartheta_j) \hat{\mathbf{p}}_{0,j,1} + \right. \right. \right. \\ \left. \left. - \sin(\varphi_j) \cos(\vartheta_j) \hat{\mathbf{p}}_{0,j,2} \right) \dot{\varphi}_j^2 + \left(-\cos(\varphi_j) \cos(\vartheta_j) \hat{\mathbf{p}}_{0,j,1} - \sin(\varphi_j) \cos(\vartheta_j) \hat{\mathbf{p}}_{0,j,2} + \sin(\vartheta_j) \hat{\mathbf{p}}_{0,j,3} \right) \dot{\vartheta}_j^2 + \right. \\ \left. \left. + \left(2 \sin(\varphi_j) \sin(\vartheta_j) \hat{\mathbf{p}}_{0,j,1} - 2 \cos(\varphi_j) \sin(\vartheta_j) \hat{\mathbf{p}}_{0,j,2} \right) \dot{\varphi}_j \dot{\vartheta}_j \right] \right\} \quad (26) \end{aligned}$$

Propellant Slosh Motion

The propellant motion is being approximated by a simplified mechanical model composed of spherical pendulums. Fig. 1 shows that a single propellant slosh particle is free to move around the geometrical center of the tank at a fixed distance l_j and this formulation is generalized to include N_P number of propellant slosh particles. The derivation begins with Euler's law for each propellant slosh particle:

$$\dot{\mathbf{H}}_{T,j} = \mathbf{L}_{T,j} + m_j \ddot{\mathbf{r}}_{T/N} \times \mathbf{l}_j \quad (27)$$

Here the term $\mathbf{L}_{T,j}$ represents the external torques. It contains the damping term that is modeled as \mathbf{D} damping matrix multiplied by the relative velocity between the tank and the propellant, \mathbf{l}'_j . It takes into account the torque due to gravity and any other external torque.

$$\mathbf{L}_{T,j} = \mathbf{l}_j \times \mathbf{F}_g - \mathbf{D}\mathbf{l}'_j + \boldsymbol{\tau}_{ext,j} \quad (28)$$

It is necessary to express \mathbf{H}_T of the propellant slosh particle as:

$$\mathbf{H}_{T,j} = m_j \mathbf{l}_j \times \dot{\mathbf{l}}_j \quad (29)$$

Deriving this equation obtains:

$$\dot{\mathbf{H}}_{T,j} = m_j \mathbf{l}_j \times \ddot{\mathbf{l}}_j \quad (30)$$

Using the transport theorem once again:

$$\ddot{\mathbf{l}}_j = \mathbf{l}''_j + \dot{\boldsymbol{\omega}}_{B/N} \times \mathbf{l}_j + 2\boldsymbol{\omega}_{B/N} \times \mathbf{l}'_j + \boldsymbol{\omega}_{B/N} \times (\boldsymbol{\omega}_{B/N} \times \mathbf{l}_j) \quad (31)$$

\mathbf{l}_j prime and second derivative are equal to (7) and (8) because the \mathbf{d} vector is constant in body frame. In fact, the following relations apply between the vectors \mathbf{l}_j and $\mathbf{r}_{P_{c,j}/B}$:

$$\mathbf{l}_j = \mathbf{r}_{P_{c,j}/B} - \mathbf{d} \quad \mathbf{l}'_j = \mathbf{r}'_{P_{c,j}/B} \quad \mathbf{l}''_j = \mathbf{r}''_{P_{c,j}/B} \quad (32)$$

Equating Eqs. (27) and (30) and using Eq. (31), yields:

$$m_j \mathbf{l}_j \times \left[\mathbf{l}''_j + \dot{\boldsymbol{\omega}}_{B/N} \times \mathbf{l}_j + 2\boldsymbol{\omega}_{B/N} \times \mathbf{l}'_j + \boldsymbol{\omega}_{B/N} \times (\boldsymbol{\omega}_{B/N} \times \mathbf{l}_j) \right] = \mathbf{L}_{T,j} + m_j \ddot{\mathbf{r}}_{T/N} \times \mathbf{l}_j \quad (33)$$

Substituting Eq. (32) in Eq. (33):

$$\begin{aligned} m_j \mathbf{l}_j \times \left[\mathbf{l}_j \left(-\ddot{\varphi}_j \sin(\varphi_j) \cos(\vartheta_j) - \dot{\vartheta}_j \cos(\varphi_j) \sin(\vartheta_j) - \dot{\varphi}_j^2 \cos(\varphi_j) \cos(\vartheta_j) - \dot{\vartheta}_j^2 \cos(\varphi_j) \cos(\vartheta_j) \right. \right. \\ \left. \left. + 2\dot{\varphi}_j \dot{\vartheta}_j \sin(\varphi_j) \sin(\vartheta_j) \right) \hat{\mathbf{p}}_{0j,1} + \mathbf{l}_j \left(\ddot{\varphi}_j \cos(\varphi_j) \cos(\vartheta_j) - \ddot{\vartheta}_j \sin(\varphi_j) \sin(\vartheta_j) - \dot{\varphi}_j^2 \sin(\varphi_j) \cos(\vartheta_j) \right. \right. \\ \left. \left. - \dot{\vartheta}_j^2 \sin(\varphi_j) \cos(\vartheta_j) - 2\dot{\varphi}_j \dot{\vartheta}_j \cos(\varphi_j) \sin(\vartheta_j) \right) \hat{\mathbf{p}}_{0j,2} + \mathbf{l}_j \left(-\ddot{\vartheta}_j \cos(\vartheta_j) + \dot{\vartheta}_j^2 \sin(\vartheta_j) \right) \hat{\mathbf{p}}_{0j,3} \right. \\ \left. + \dot{\boldsymbol{\omega}}_{B/N} \times \mathbf{l}_j + 2\boldsymbol{\omega}_{B/N} \times \mathbf{l}'_j + \boldsymbol{\omega}_{B/N} \times (\boldsymbol{\omega}_{B/N} \times \mathbf{l}_j) \right] = \mathbf{L}_{T,j} + m_j \ddot{\mathbf{r}}_{T/N} \times \mathbf{l}_j \quad (34) \end{aligned}$$

Executing the vectorial products and projecting Eq. (34) on the axis of rotation of φ and ϑ , the propellant slosh particle equations are obtained. Fig. 3 shows the rotations axes on which the Eq. (34) is projected. The φ rotation axis is $\hat{\mathbf{p}}_{0j,3}$, while is called $\hat{\mathbf{p}}'_{0j,2}$ the ϑ rotation axis.

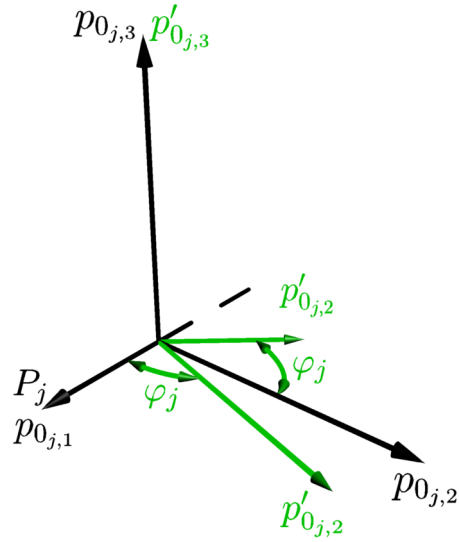


Figure 3: Rotation Axes

$$\hat{\mathbf{p}}_{0,j,3} = \begin{matrix} \mathcal{P}_{0,j} \\ \begin{bmatrix} 0 \\ 0 \\ 1 \end{bmatrix} \end{matrix} \quad (35)$$

$$m_j l_j^2 \left[\ddot{\varphi}_j \cos^2(\vartheta_j) - 2\dot{\varphi}_j \dot{\vartheta}_j \cos(\vartheta_j) \sin(\vartheta_j) \right] + m_j \hat{\mathbf{p}}_{0,j,3}^T \mathbf{l}_j \times \left[\dot{\boldsymbol{\omega}}_{B/N} \times \mathbf{l}_j + 2\boldsymbol{\omega}_{B/N} \times \mathbf{l}'_j + \boldsymbol{\omega}_{B/N} \times (\boldsymbol{\omega}_{B/N} \times \mathbf{l}_j) \right] = \hat{\mathbf{p}}_{0,j,3}^T \mathbf{L}_{T,j} + m_j \hat{\mathbf{p}}_{0,j,3}^T \ddot{\mathbf{r}}_{T/N} \times \mathbf{l}_j \quad (36)$$

$$\hat{\mathbf{p}}'_{0,j,2} = \begin{matrix} \mathcal{P}_{0,j} \\ \begin{bmatrix} -\sin(\varphi) \\ \cos(\varphi) \\ 0 \end{bmatrix} \end{matrix} \quad (37)$$

$$m_j l_j^2 \left[\ddot{\vartheta}_j + \dot{\varphi}_j^2 \cos(\vartheta_j) \sin(\vartheta_j) \right] + m_j \hat{\mathbf{p}}'_{0,j,2}{}^T \mathbf{l}_j \times \left[\dot{\boldsymbol{\omega}}_{B/N} \times \mathbf{l}_j + 2\boldsymbol{\omega}_{B/N} \times \mathbf{l}'_j + \boldsymbol{\omega}_{B/N} \times (\boldsymbol{\omega}_{B/N} \times \mathbf{l}_j) \right] = \hat{\mathbf{p}}'_{0,j,2}{}^T \mathbf{L}_{T,j} + m_j \hat{\mathbf{p}}'_{0,j,2}{}^T \ddot{\mathbf{r}}_{T/N} \times \mathbf{l}_j \quad (38)$$

Remembering that $\mathbf{r}_{T/N} = \mathbf{r}_{B/N} + \mathbf{d}$, and that \mathbf{d} is constant in the body frame, the transport theorem is used to write:

$$\ddot{\mathbf{d}} = \dot{\boldsymbol{\omega}}_{B/N} \times \mathbf{d} + \boldsymbol{\omega}_{B/N} \times (\boldsymbol{\omega}_{B/N} \times \mathbf{d}) \quad (39)$$

$$\ddot{\mathbf{r}}_{T/N} = \ddot{\mathbf{r}}_{B/N} + \dot{\boldsymbol{\omega}}_{B/N} \times \mathbf{d} + \boldsymbol{\omega}_{B/N} \times (\boldsymbol{\omega}_{B/N} \times \mathbf{d}) \quad (40)$$

Rearranging the terms as done in the previous sections:

$$m_j l_j^2 \ddot{\varphi}_j \cos^2(\vartheta_j) - m_j \hat{\mathbf{p}}_{0,j,3}^T [\tilde{\mathbf{l}}_j] ([\tilde{\mathbf{l}}_j] + [\tilde{\mathbf{d}}]) \dot{\boldsymbol{\omega}}_{B/N} + m_j \hat{\mathbf{p}}_{0,j,3}^T [\tilde{\mathbf{l}}_j] \ddot{\mathbf{r}}_{B/N} = -m_j \hat{\mathbf{p}}_{0,j,3}^T [\tilde{\mathbf{l}}_j] [\tilde{\boldsymbol{\omega}}_{B/N}] [\tilde{\boldsymbol{\omega}}_{B/N}] \mathbf{d} + \hat{\mathbf{p}}_{0,j,3}^T \mathbf{L}_{T,j} + 2m_j l_j^2 \dot{\varphi}_j \dot{\vartheta}_j \cos(\vartheta_j) \sin(\vartheta_j) - m_j \hat{\mathbf{p}}_{0,j,3}^T [\tilde{\mathbf{l}}_j] \left[2[\tilde{\boldsymbol{\omega}}_{B/N}] \mathbf{l}'_j + [\tilde{\boldsymbol{\omega}}_{B/N}] [\tilde{\boldsymbol{\omega}}_{B/N}] \mathbf{l}_j \right] \quad (41)$$

$$\begin{aligned}
m_j l_j^2 \ddot{\vartheta}_j - m_j \hat{\mathbf{p}}_{0,j,2}'^T [\tilde{\mathbf{l}}_j] ([\tilde{\mathbf{l}}_j] + [\tilde{\mathbf{d}}]) \dot{\boldsymbol{\omega}}_{B/N} + m_j \hat{\mathbf{p}}_{0,j,2}'^T [\tilde{\mathbf{l}}_j] \ddot{\mathbf{r}}_{B/N} = -m_j \hat{\mathbf{p}}_{0,j,2}'^T [\tilde{\mathbf{l}}_j] [\tilde{\boldsymbol{\omega}}_{B/N}] [\tilde{\boldsymbol{\omega}}_{B/N}] \mathbf{d} \\
+ \hat{\mathbf{p}}_{0,j,2}'^T \mathbf{L}_{T,j} - m_j l_j^2 \dot{\varphi}_j^2 \cos(\vartheta_j) \sin(\vartheta_j) - m_j \hat{\mathbf{p}}_{0,j,2}'^T [\tilde{\mathbf{l}}_j] \left[2[\tilde{\boldsymbol{\omega}}_{B/N}] \mathbf{l}'_j + [\tilde{\boldsymbol{\omega}}_{B/N}] [\tilde{\boldsymbol{\omega}}_{B/N}] \mathbf{l}_j \right]
\end{aligned} \tag{42}$$

Eqs. (41) and (42) are the Propellant Slosh Particle equations. In the next section the EOMs obtained so far are further manipulated to derive the back substitution method which increase the efficiency of the software in terms of computing time.

BACK-SUBSTITUTION METHOD

The EOMs obtained in the previous sections constitute a system of $2N_P + 6$ coupled differential equations. Therefore, to numerically integrate the EOMs, it would be necessary to invert a system mass matrix of size $2N_P + 6$. This can result in a computationally expensive simulation. The computation effort to numerically invert an $N \times N$ matrix scales with N^3 .¹⁶ Implementing a back-substitution method is possible to reduce considerably the computing cost.¹⁰ In the following sections, it is demonstrated how the problem is reduced to an inversion of two (3×3) matrices. As it is shown in Eqs. (65) and (66),¹⁰ the A^{-1} and $(D - CA^{-1}B)^{-1}$ are the two matrices to be inverted. Then the system is completely solved back substituting for propellant slosh and translational motions. A step-by-step derivation of the back-substitution method is presented in the following sections.

Propellant Slosh Motion

The spherical pendulum equation have a complex expression that needs to be simplified to decouple the propellant slosh particle from the proper motion of the spacecraft. In this section, the angular accelerations, that control the pendulum motion, are isolated from the other variables that control the motion.

Starting from inverting Eq. (41) to obtain the expression of $\ddot{\varphi}_j$:

$$\begin{aligned}
\ddot{\varphi}_j = \frac{1}{m_j l_j^2 \cos^2(\vartheta_j)} \left\{ m_j \hat{\mathbf{p}}_{0,j,3}^T [\tilde{\mathbf{l}}_j] ([\tilde{\mathbf{l}}_j] + [\tilde{\mathbf{d}}]) \dot{\boldsymbol{\omega}}_{B/N} - m_j \hat{\mathbf{p}}_{0,j,3}^T [\tilde{\mathbf{l}}_j] \ddot{\mathbf{r}}_{B/N} - m_j \hat{\mathbf{p}}_{0,j,3}^T [\tilde{\mathbf{l}}_j] [\tilde{\boldsymbol{\omega}}_{B/N}] [\tilde{\boldsymbol{\omega}}_{B/N}] \mathbf{d} \right. \\
\left. + \hat{\mathbf{p}}_{0,j,3}^T \mathbf{L}_{T,j} + 2m_j l_j^2 \dot{\varphi}_j \dot{\vartheta} \cos(\vartheta_j) \sin(\vartheta_j) - m_j \hat{\mathbf{p}}_{0,j,3}^T [\tilde{\mathbf{l}}_j] \left[2[\tilde{\boldsymbol{\omega}}_{B/N}] \mathbf{l}'_j + [\tilde{\boldsymbol{\omega}}_{B/N}] [\tilde{\boldsymbol{\omega}}_{B/N}] \mathbf{l}_j \right] \right\} \tag{43}
\end{aligned}$$

$$\ddot{\varphi}_j = \frac{1}{m_j l_j^2 \cos^2(\vartheta_j)} \left(m_j \hat{\mathbf{p}}_{0,j,3}^T [\tilde{\mathbf{l}}_j] ([\tilde{\mathbf{l}}_j] + [\tilde{\mathbf{d}}]) \dot{\boldsymbol{\omega}}_{B/N} - m_j \hat{\mathbf{p}}_{0,j,3}^T [\tilde{\mathbf{l}}_j] \ddot{\mathbf{r}}_{B/N} + a_{\varphi_j} \right) \tag{44}$$

Introducing a new notation to make the equations shorter, lets us to appreciate better the dependence of the propellant slosh particle from the other variables that control the spacecraft motion:

$$\ddot{\varphi}_j = \mathbf{a}_{\varphi_j}^T \ddot{\mathbf{r}}_{B/N} + \mathbf{b}_{\varphi_j}^T \dot{\boldsymbol{\omega}}_{B/N} + c_{\varphi_j} \tag{45}$$

with the following definitions:

$$\mathbf{a}_{\varphi_j}^T = -\frac{\hat{\mathbf{p}}_{0,j,3}^T[\tilde{\mathbf{l}}_j]}{l_j^2 \cos^2(\vartheta_j)} \quad (46)$$

$$\mathbf{b}_{\varphi_j}^T = \frac{\hat{\mathbf{p}}_{0,j,3}^T\tilde{\mathbf{l}}_j + [\tilde{\mathbf{d}}]}{l_j^2 \cos^2(\vartheta_j)} \quad (47)$$

$$c_{\varphi_j} = \frac{1}{m_j l_j^2 \cos^2(\vartheta_j)} \left\{ -m_j \hat{\mathbf{p}}_{0,j,3}^T[\tilde{\mathbf{l}}_j][\tilde{\boldsymbol{\omega}}_{\mathcal{B}/\mathcal{N}}][\tilde{\boldsymbol{\omega}}_{\mathcal{B}/\mathcal{N}}]\mathbf{d} + \hat{\mathbf{p}}_{0,j,3}^T \mathbf{L}_{T,j} \right. \\ \left. + 2m_j l_j^2 \dot{\varphi}_j \dot{\vartheta} \cos(\vartheta_j) \sin(\vartheta_j) - m_j \hat{\mathbf{p}}_{0,j,3}^T[\tilde{\mathbf{l}}_j] \left[2[\tilde{\boldsymbol{\omega}}_{\mathcal{B}/\mathcal{N}}]\mathbf{l}'_j + [\tilde{\boldsymbol{\omega}}_{\mathcal{B}/\mathcal{N}}][\tilde{\boldsymbol{\omega}}_{\mathcal{B}/\mathcal{N}}]\mathbf{l}_j \right] \right\} \quad (48)$$

Performing the same operations for Eq. (42) to isolate $\ddot{\vartheta}_j$:

$$\ddot{\vartheta}_j = \frac{1}{m_j l_j^2} \left\{ m_j \hat{\mathbf{p}}_{0,j,2}'^T\tilde{\mathbf{l}}_j + [\tilde{\mathbf{d}}] \dot{\boldsymbol{\omega}}_{\mathcal{B}/\mathcal{N}} - m_j \hat{\mathbf{p}}_{0,j,2}'^T[\tilde{\mathbf{l}}_j] \ddot{\mathbf{r}}_{\mathcal{B}/\mathcal{N}} - m_j \hat{\mathbf{p}}_{0,j,2}'^T[\tilde{\mathbf{l}}_j][\tilde{\boldsymbol{\omega}}_{\mathcal{B}/\mathcal{N}}][\tilde{\boldsymbol{\omega}}_{\mathcal{B}/\mathcal{N}}]\mathbf{d} \right. \\ \left. + \hat{\mathbf{p}}_{0,j,2}'^T \mathbf{L}_{T,j} - m_j l_j^2 \dot{\varphi}_j^2 \cos(\vartheta_j) \sin(\vartheta_j) - m_j \hat{\mathbf{p}}_{0,j,2}'^T[\tilde{\mathbf{l}}_j] \left[2[\tilde{\boldsymbol{\omega}}_{\mathcal{B}/\mathcal{N}}]\mathbf{l}'_j + [\tilde{\boldsymbol{\omega}}_{\mathcal{B}/\mathcal{N}}][\tilde{\boldsymbol{\omega}}_{\mathcal{B}/\mathcal{N}}]\mathbf{l}_j \right] \right\} \quad (49)$$

$$\ddot{\vartheta}_j = \frac{1}{m_j l_j^2} \left(m_j \hat{\mathbf{p}}_{0,j,2}'^T\tilde{\mathbf{l}}_j + [\tilde{\mathbf{d}}] \dot{\boldsymbol{\omega}}_{\mathcal{B}/\mathcal{N}} - m_j \hat{\mathbf{p}}_{0,j,2}'^T[\tilde{\mathbf{l}}_j] \ddot{\mathbf{r}}_{\mathcal{B}/\mathcal{N}} + a_{\vartheta_j} \right) \quad (50)$$

Writing this a different way, following the procedure used for $\ddot{\varphi}_j$, yields the final back-substitution contributions of the spherical pendulum:

$$\ddot{\vartheta}_j = \mathbf{a}_{\vartheta_j}^T \ddot{\mathbf{r}}_{\mathcal{B}/\mathcal{N}} + \mathbf{b}_{\vartheta_j}^T \dot{\boldsymbol{\omega}}_{\mathcal{B}/\mathcal{N}} + c_{\vartheta_j} \quad (51)$$

$$\mathbf{a}_{\vartheta_j}^T = -\frac{\hat{\mathbf{p}}_{0,j,2}'^T[\tilde{\mathbf{l}}_j]}{l_j^2} \quad (52)$$

$$\mathbf{b}_{\vartheta_j}^T = \frac{\hat{\mathbf{p}}_{0,j,2}'^T\tilde{\mathbf{l}}_j + [\tilde{\mathbf{d}}]}{l_j^2} \quad (53)$$

$$c_{\vartheta_j} = \frac{1}{m_j l_j^2} \left\{ -m_j \hat{\mathbf{p}}_{0,j,2}'^T[\tilde{\mathbf{l}}_j][\tilde{\boldsymbol{\omega}}_{\mathcal{B}/\mathcal{N}}][\tilde{\boldsymbol{\omega}}_{\mathcal{B}/\mathcal{N}}]\mathbf{d} + \hat{\mathbf{p}}_{0,j,2}'^T \mathbf{L}_{T,j} - m_j l_j^2 \dot{\varphi}_j^2 \cos(\vartheta_j) \sin(\vartheta_j) \right. \\ \left. - m_j \hat{\mathbf{p}}_{0,j,2}'^T[\tilde{\mathbf{l}}_j] \left[2[\tilde{\boldsymbol{\omega}}_{\mathcal{B}/\mathcal{N}}]\mathbf{l}'_j + [\tilde{\boldsymbol{\omega}}_{\mathcal{B}/\mathcal{N}}][\tilde{\boldsymbol{\omega}}_{\mathcal{B}/\mathcal{N}}]\mathbf{l}_j \right] \right\} \quad (54)$$

Translational and Rotational EOMs Manipulation

The translational and rotational EOMs can now be updated with the new form of the propellant slosh equation, obtained in the previous section. These are the key passages of the back-substitution method that enables the desired fast computation.

Plugging these definitions into the translation and rotational equations of motion and multiplying by m_{sc} , Eq. (14) and (26) result in:

$$\begin{aligned}
& \left\{ [I_{3 \times 3}] - \frac{1}{m_{sc}} \sum_{j=1}^{N_P} m_j l_j \left[\left(\sin(\varphi_j) \cos(\vartheta_j) \hat{\mathbf{p}}_{0,j,1} - \cos(\varphi_j) \cos(\vartheta_j) \hat{\mathbf{p}}_{0,j,2} \right) \mathbf{a}_{\varphi_j}^T + \left(\cos(\varphi_j) \sin(\vartheta_j) \hat{\mathbf{p}}_{0,j,1} \right. \right. \right. \\
& + \left. \left. \sin(\varphi_j) \sin(\vartheta_j) \hat{\mathbf{p}}_{0,j,2} + \cos(\vartheta_j) \hat{\mathbf{p}}_{0,j,3} \right) \mathbf{a}_{\vartheta_j}^T \right] \right\} \ddot{\mathbf{r}}_{B/N} + \left\{ -[\tilde{\mathbf{c}}] - \frac{1}{m_{sc}} \sum_{j=1}^{N_P} m_j l_j \left[\left(\sin(\varphi_j) \cos(\vartheta_j) \hat{\mathbf{p}}_{0,j,1} \right. \right. \right. \\
& - \left. \left. \cos(\varphi_j) \cos(\vartheta_j) \hat{\mathbf{p}}_{0,j,2} \right) \mathbf{b}_{\varphi_j}^T + \left(\cos(\varphi_j) \sin(\vartheta_j) \hat{\mathbf{p}}_{0,j,1} + \sin(\varphi_j) \sin(\vartheta_j) \hat{\mathbf{p}}_{0,j,2} + \cos(\vartheta_j) \hat{\mathbf{p}}_{0,j,3} \right) \mathbf{b}_{\vartheta_j}^T \right] \right\} \dot{\boldsymbol{\omega}}_{B/N} \\
& = \ddot{\mathbf{r}}_{C/N} - 2[\tilde{\boldsymbol{\omega}}_{B/N}] \mathbf{c}' - [\tilde{\boldsymbol{\omega}}_{B/N}][\tilde{\boldsymbol{\omega}}_{B/N}] \mathbf{c} - \frac{1}{m_{sc}} \sum_{j=1}^{N_P} m_j l_j \left[\left(-\cos(\varphi_j) \cos(\vartheta_j) \hat{\mathbf{p}}_{0,j,1} \right. \right. \\
& - \left. \left. \sin(\varphi_j) \cos(\vartheta_j) \hat{\mathbf{p}}_{0,j,2} \right) \dot{\varphi}_j^2 + \left(-\cos(\varphi_j) \cos(\vartheta_j) \hat{\mathbf{p}}_{0,j,1} - \sin(\varphi_j) \cos(\vartheta_j) \hat{\mathbf{p}}_{0,j,2} + \sin(\vartheta_j) \hat{\mathbf{p}}_{0,j,3} \right) \dot{\vartheta}_j^2 \right. \\
& + \left. \left(2 \sin(\varphi_j) \sin(\vartheta_j) \hat{\mathbf{p}}_{0,j,1} - 2 \cos(\varphi_j) \sin(\vartheta_j) \hat{\mathbf{p}}_{0,j,2} \right) \dot{\varphi}_j \dot{\vartheta}_j - \left(\sin(\varphi_j) \cos(\vartheta_j) \hat{\mathbf{p}}_{0,j,1} \right. \right. \\
& \left. \left. - \cos(\varphi_j) \cos(\vartheta_j) \hat{\mathbf{p}}_{0,j,2} \right) c_{\varphi_j} - \left(\cos(\varphi_j) \sin(\vartheta_j) \hat{\mathbf{p}}_{0,j,1} + \sin(\varphi_j) \sin(\vartheta_j) \hat{\mathbf{p}}_{0,j,2} + \cos(\vartheta_j) \hat{\mathbf{p}}_{0,j,3} \right) c_{\vartheta_j} \right] \\
& \tag{55}
\end{aligned}$$

Multiply both sides by m_{sc} :

$$\begin{aligned}
& \left\{ m_{sc} [I_{3 \times 3}] - \sum_{j=1}^{N_P} m_j l_j \left[\left(\sin(\varphi_j) \cos(\vartheta_j) \hat{\mathbf{p}}_{0,j,1} - \cos(\varphi_j) \cos(\vartheta_j) \hat{\mathbf{p}}_{0,j,2} \right) \mathbf{a}_{\varphi_j}^T + \left(\cos(\varphi_j) \sin(\vartheta_j) \hat{\mathbf{p}}_{0,j,1} \right. \right. \right. \\
& + \left. \left. \sin(\varphi_j) \sin(\vartheta_j) \hat{\mathbf{p}}_{0,j,2} + \cos(\vartheta_j) \hat{\mathbf{p}}_{0,j,3} \right) \mathbf{a}_{\vartheta_j}^T \right] \right\} \ddot{\mathbf{r}}_{B/N} + \left\{ -m_{sc} [\tilde{\mathbf{c}}] - \sum_{j=1}^{N_P} m_j l_j \left[\left(\sin(\varphi_j) \cos(\vartheta_j) \hat{\mathbf{p}}_{0,j,1} \right. \right. \right. \\
& - \left. \left. \cos(\varphi_j) \cos(\vartheta_j) \hat{\mathbf{p}}_{0,j,2} \right) \mathbf{b}_{\varphi_j}^T + \left(\cos(\varphi_j) \sin(\vartheta_j) \hat{\mathbf{p}}_{0,j,1} + \sin(\varphi_j) \sin(\vartheta_j) \hat{\mathbf{p}}_{0,j,2} + \cos(\vartheta_j) \hat{\mathbf{p}}_{0,j,3} \right) \mathbf{b}_{\vartheta_j}^T \right] \right\} \dot{\boldsymbol{\omega}}_{B/N} \\
& = m_{sc} \ddot{\mathbf{r}}_{C/N} - 2m_{sc} [\tilde{\boldsymbol{\omega}}_{B/N}] \mathbf{c}' - m_{sc} [\tilde{\boldsymbol{\omega}}_{B/N}][\tilde{\boldsymbol{\omega}}_{B/N}] \mathbf{c} - \sum_{j=1}^{N_P} m_j l_j \left[\left(-\cos(\varphi_j) \cos(\vartheta_j) \hat{\mathbf{p}}_{0,j,1} \right. \right. \\
& - \left. \left. \sin(\varphi_j) \cos(\vartheta_j) \hat{\mathbf{p}}_{0,j,2} \right) \dot{\varphi}_j^2 + \left(-\cos(\varphi_j) \cos(\vartheta_j) \hat{\mathbf{p}}_{0,j,1} - \sin(\varphi_j) \cos(\vartheta_j) \hat{\mathbf{p}}_{0,j,2} + \sin(\vartheta_j) \hat{\mathbf{p}}_{0,j,3} \right) \dot{\vartheta}_j^2 \right. \\
& + \left. \left(2 \sin(\varphi_j) \sin(\vartheta_j) \hat{\mathbf{p}}_{0,j,1} - 2 \cos(\varphi_j) \sin(\vartheta_j) \hat{\mathbf{p}}_{0,j,2} \right) \dot{\varphi}_j \dot{\vartheta}_j - \left(\sin(\varphi_j) \cos(\vartheta_j) \hat{\mathbf{p}}_{0,j,1} \right. \right. \\
& \left. \left. - \cos(\varphi_j) \cos(\vartheta_j) \hat{\mathbf{p}}_{0,j,2} \right) c_{\varphi_j} - \left(\cos(\varphi_j) \sin(\vartheta_j) \hat{\mathbf{p}}_{0,j,1} + \sin(\varphi_j) \sin(\vartheta_j) \hat{\mathbf{p}}_{0,j,2} + \cos(\vartheta_j) \hat{\mathbf{p}}_{0,j,3} \right) c_{\vartheta_j} \right] \\
& \tag{56}
\end{aligned}$$

Rotational EOM Manipulation

Performing the same operations for the second EOM, Eq (26) becomes:

$$\left\{ m_{sc} [\tilde{\mathbf{c}}] - \sum_{j=1}^{N_P} m_j l_j [\tilde{\mathbf{r}}_{P_{c,j}/B}] \left[\left(\sin(\varphi_j) \cos(\vartheta_j) \hat{\mathbf{p}}_{0,j,1} - \cos(\varphi_j) \cos(\vartheta_j) \hat{\mathbf{p}}_{0,j,2} \right) \mathbf{a}_{\varphi_j}^T + \left(\cos(\varphi_j) \sin(\vartheta_j) \hat{\mathbf{p}}_{0,j,1} \right. \right. \right.$$

$$\begin{aligned}
& + \sin(\varphi_j) \sin(\vartheta_j) \hat{\mathbf{p}}_{0,j,2} + \cos(\vartheta_j) \hat{\mathbf{p}}_{0,j,3} \mathbf{a}_{\vartheta_j}^T \Big] \ddot{\mathbf{r}}_{B/N} + \left\{ [I_{sc,B}] - \sum_{j=1}^{N_P} m_j l_j [\tilde{\mathbf{r}}_{P_{c,j}/B}] \left[\left(\sin(\varphi_j) \cos(\vartheta_j) \hat{\mathbf{p}}_{0,j,1} \right. \right. \right. \\
& \left. \left. \left. - \cos(\varphi_j) \cos(\vartheta_j) \hat{\mathbf{p}}_{0,j,2} \right) \mathbf{b}_{\varphi_j}^T + \left(\cos(\varphi_j) \sin(\vartheta_j) \hat{\mathbf{p}}_{0,j,1} + \sin(\varphi_j) \sin(\vartheta_j) \hat{\mathbf{p}}_{0,j,2} + \cos(\vartheta_j) \hat{\mathbf{p}}_{0,j,3} \right) \mathbf{b}_{\vartheta_j}^T \right] \right\} \dot{\boldsymbol{\omega}}_{B/N} \\
& = \mathbf{L}_B - [\tilde{\boldsymbol{\omega}}_{B/N}] [I_{sc,B}] \boldsymbol{\omega}_{B/N} - [I'_{sc,B}] \boldsymbol{\omega}_{B/N} - \sum_{j=1}^{N_P} m_j \left\{ [\tilde{\boldsymbol{\omega}}_{B/N}] [\tilde{\mathbf{r}}_{P_{c,j}/B}] \mathbf{r}'_{P_{c,j}/B} \right. \\
& + l_j [\tilde{\mathbf{r}}_{P_{c,j}/B}] \left[\left(-\cos(\varphi_j) \cos(\vartheta_j) \hat{\mathbf{p}}_{0,j,1} - \sin(\varphi_j) \cos(\vartheta_j) \hat{\mathbf{p}}_{0,j,2} \right) \dot{\varphi}_j^2 + \left(-\cos(\varphi_j) \cos(\vartheta_j) \hat{\mathbf{p}}_{0,j,1} \right. \right. \\
& \quad \left. \left. - \sin(\varphi_j) \cos(\vartheta_j) \hat{\mathbf{p}}_{0,j,2} + \sin(\vartheta_j) \hat{\mathbf{p}}_{0,j,3} \right) \dot{\vartheta}_j^2 + \left(2 \sin(\varphi_j) \sin(\vartheta_j) \hat{\mathbf{p}}_{0,j,1} \right. \right. \\
& \quad \left. \left. - 2 \cos(\varphi_j) \sin(\vartheta_j) \hat{\mathbf{p}}_{0,j,2} \right) \dot{\varphi}_j \dot{\vartheta}_j - \left(\sin(\varphi_j) \cos(\vartheta_j) \hat{\mathbf{p}}_{0,j,1} - \cos(\varphi_j) \cos(\vartheta_j) \hat{\mathbf{p}}_{0,j,2} \right) c_{\varphi_j} \right. \\
& \quad \left. - \left(\cos(\varphi_j) \sin(\vartheta_j) \hat{\mathbf{p}}_{0,j,1} + \sin(\varphi_j) \sin(\vartheta_j) \hat{\mathbf{p}}_{0,j,2} + \cos(\vartheta_j) \hat{\mathbf{p}}_{0,j,3} \right) c_{\vartheta_j} \right] \Big\} \quad (57)
\end{aligned}$$

These equations provide the required back-substitution contributions. As is evident above, performing the back-substitution instead of a numerical inverse of the system mass matrix is challenging and complex to formulate. However, once this solution is found, it can be readily applied to a range of complex spacecraft dynamics without having to re-derive the associated equations of motion.

Remaining Back-substitution Steps

In this section, the final steps to complete the back-substitution method procedure are presented. Here, the equation are manipulated again to obtain a final form of the system which is easy to read and implement in the software, providing also a short computing time.

The required back-substitution contributions of the spherical pendulum model are summarized as:

$$\begin{aligned}
[A] = \left\{ m_{sc} [I_{3 \times 3}] - \sum_{j=1}^{N_P} m_j l_j \left[\left(\sin(\varphi_j) \cos(\vartheta_j) \hat{\mathbf{p}}_{0,j,1} - \cos(\varphi_j) \cos(\vartheta_j) \hat{\mathbf{p}}_{0,j,2} \right) \mathbf{a}_{\varphi_j}^T \right. \right. \\
\left. \left. + \left(\cos(\varphi_j) \sin(\vartheta_j) \hat{\mathbf{p}}_{0,j,1} + \sin(\varphi_j) \sin(\vartheta_j) \hat{\mathbf{p}}_{0,j,2} + \cos(\vartheta_j) \hat{\mathbf{p}}_{0,j,3} \right) \mathbf{a}_{\vartheta_j}^T \right] \right\} \quad (58)
\end{aligned}$$

$$\begin{aligned}
[B] = \left\{ -m_{sc} [\tilde{\mathbf{c}}] - \sum_{j=1}^{N_P} m_j l_j \left[\left(\sin(\varphi_j) \cos(\vartheta_j) \hat{\mathbf{p}}_{0,j,1} - \cos(\varphi_j) \cos(\vartheta_j) \hat{\mathbf{p}}_{0,j,2} \right) \mathbf{b}_{\varphi_j}^T \right. \right. \\
\left. \left. + \left(\cos(\varphi_j) \sin(\vartheta_j) \hat{\mathbf{p}}_{0,j,1} + \sin(\varphi_j) \sin(\vartheta_j) \hat{\mathbf{p}}_{0,j,2} + \cos(\vartheta_j) \hat{\mathbf{p}}_{0,j,3} \right) \mathbf{b}_{\vartheta_j}^T \right] \right\} \quad (59)
\end{aligned}$$

$$\begin{aligned}
[C] = \left\{ m_{sc} [\tilde{\mathbf{c}}] - \sum_{j=1}^{N_P} m_j l_j [\tilde{\mathbf{r}}_{P_{c,j}/B}] \left[\left(\sin(\varphi_j) \cos(\vartheta_j) \hat{\mathbf{p}}_{0,j,1} - \cos(\varphi_j) \cos(\vartheta_j) \hat{\mathbf{p}}_{0,j,2} \right) \mathbf{a}_{\varphi_j}^T \right. \right. \\
\left. \left. + \left(\cos(\varphi_j) \sin(\vartheta_j) \hat{\mathbf{p}}_{0,j,1} + \sin(\varphi_j) \sin(\vartheta_j) \hat{\mathbf{p}}_{0,j,2} + \cos(\vartheta_j) \hat{\mathbf{p}}_{0,j,3} \right) \mathbf{a}_{\vartheta_j}^T \right] \right\} \quad (60)
\end{aligned}$$

$$[D] = \left\{ [I_{\text{sc},B}] - \sum_{j=1}^{N_P} m_j l_j [\tilde{\mathbf{r}}_{P_{c,j}/B}] \left[\left(\sin(\varphi_j) \cos(\vartheta_j) \hat{\mathbf{p}}_{0,j,1} - \cos(\varphi_j) \cos(\vartheta_j) \hat{\mathbf{p}}_{0,j,2} \right) \mathbf{b}_{\varphi_j}^T \right. \right. \\ \left. \left. + \left(\cos(\varphi_j) \sin(\vartheta_j) \hat{\mathbf{p}}_{0,j,1} + \sin(\varphi_j) \sin(\vartheta_j) \hat{\mathbf{p}}_{0,j,2} + \cos(\vartheta_j) \hat{\mathbf{p}}_{0,j,3} \right) \mathbf{b}_{\vartheta_j}^T \right] \right\} \quad (61)$$

$$\mathbf{v}_{\text{trans}} = m_{\text{sc}} \ddot{\mathbf{r}}_{C/N} - 2m_{\text{sc}} [\tilde{\boldsymbol{\omega}}_{B/N}] \mathbf{c}' - m_{\text{sc}} [\tilde{\boldsymbol{\omega}}_{B/N}] [\tilde{\boldsymbol{\omega}}_{B/N}] \mathbf{c} \\ - \sum_{j=1}^{N_P} m_j l_j \left[\left(-\cos(\varphi_j) \cos(\vartheta_j) \hat{\mathbf{p}}_{0,j,1} - \sin(\varphi_j) \cos(\vartheta_j) \hat{\mathbf{p}}_{0,j,2} \right) \dot{\varphi}_j^2 + \left(-\cos(\varphi_j) \cos(\vartheta_j) \hat{\mathbf{p}}_{0,j,1} \right. \right. \\ \left. \left. - \sin(\varphi_j) \cos(\vartheta_j) \hat{\mathbf{p}}_{0,j,2} + \sin(\vartheta_j) \hat{\mathbf{p}}_{0,j,3} \right) \dot{\vartheta}_j^2 + \left(2 \sin(\varphi_j) \sin(\vartheta_j) \hat{\mathbf{p}}_{0,j,1} \right. \right. \\ \left. \left. - 2 \cos(\varphi_j) \sin(\vartheta_j) \hat{\mathbf{p}}_{0,j,2} \right) \dot{\varphi}_j \dot{\vartheta}_j - \left(\sin(\varphi_j) \cos(\vartheta_j) \hat{\mathbf{p}}_{0,j,1} - \cos(\varphi_j) \cos(\vartheta_j) \hat{\mathbf{p}}_{0,j,2} \right) c_{\varphi_j} \right. \\ \left. - \left(\cos(\varphi_j) \sin(\vartheta_j) \hat{\mathbf{p}}_{0,j,1} + \sin(\varphi_j) \sin(\vartheta_j) \hat{\mathbf{p}}_{0,j,2} + \cos(\vartheta_j) \hat{\mathbf{p}}_{0,j,3} \right) c_{\vartheta_j} \right] \quad (62)$$

$$\mathbf{v}_{\text{rot}} = \mathbf{L}_B - [\tilde{\boldsymbol{\omega}}_{B/N}] [I_{\text{sc},B}] \boldsymbol{\omega}_{B/N} - [I'_{\text{sc},B}] \boldsymbol{\omega}_{B/N} \\ - \sum_{j=1}^{N_P} m_j \left\{ [\tilde{\boldsymbol{\omega}}_{B/N}] [\tilde{\mathbf{r}}_{P_{c,j}/B}] \mathbf{r}'_{P_{c,j}/B} + l_j [\tilde{\mathbf{r}}_{P_{c,j}/B}] \left[\left(-\cos(\varphi_j) \cos(\vartheta_j) \hat{\mathbf{p}}_{0,j,1} - \sin(\varphi_j) \cos(\vartheta_j) \hat{\mathbf{p}}_{0,j,2} \right) \dot{\varphi}_j^2 \right. \right. \\ \left. \left. + \left(-\cos(\varphi_j) \cos(\vartheta_j) \hat{\mathbf{p}}_{0,j,1} - \sin(\varphi_j) \cos(\vartheta_j) \hat{\mathbf{p}}_{0,j,2} + \sin(\vartheta_j) \hat{\mathbf{p}}_{0,j,3} \right) \dot{\vartheta}_j^2 + \left(2 \sin(\varphi_j) \sin(\vartheta_j) \hat{\mathbf{p}}_{0,j,1} \right. \right. \right. \\ \left. \left. - 2 \cos(\varphi_j) \sin(\vartheta_j) \hat{\mathbf{p}}_{0,j,2} \right) \dot{\varphi}_j \dot{\vartheta}_j - \left(\sin(\varphi_j) \cos(\vartheta_j) \hat{\mathbf{p}}_{0,j,1} - \cos(\varphi_j) \cos(\vartheta_j) \hat{\mathbf{p}}_{0,j,2} \right) c_{\varphi_j} \right. \\ \left. - \left(\cos(\varphi_j) \sin(\vartheta_j) \hat{\mathbf{p}}_{0,j,1} + \sin(\varphi_j) \sin(\vartheta_j) \hat{\mathbf{p}}_{0,j,2} + \cos(\vartheta_j) \hat{\mathbf{p}}_{0,j,3} \right) c_{\vartheta_j} \right] \right\} \quad (63)$$

Therefore, the translation and rotation EOMs can be simplified and written using the above definitions:

$$\begin{bmatrix} [A] & [B] \\ [C] & [D] \end{bmatrix} \begin{bmatrix} \ddot{\mathbf{r}}_{B/N} \\ \dot{\boldsymbol{\omega}}_{B/N} \end{bmatrix} = \begin{bmatrix} \mathbf{v}_{\text{trans}} \\ \mathbf{v}_{\text{rot}} \end{bmatrix} \quad (64)$$

Solving the system-of-equations by:

$$\dot{\boldsymbol{\omega}}_{B/N} = \left([D] - [C][A]^{-1}[B] \right)^{-1} (\mathbf{v}_{\text{rot}} - [C][A]^{-1} \mathbf{v}_{\text{trans}}) \quad (65)$$

$$\ddot{\mathbf{r}}_{B/N} = [A]^{-1} (\mathbf{v}_{\text{trans}} - [B] \dot{\boldsymbol{\omega}}_{B/N}) \quad (66)$$

This demonstrates that to solve the problem with the new formulation only the is necessary to invert only A^{-1} and $(D - CA^{-1}B)^{-1}$. Now, the other state variables can be solved using Eqs. (45) and (51):

$$\ddot{\varphi}_j = \mathbf{a}_{\varphi_j}^T \ddot{\mathbf{r}}_{B/N} + \mathbf{b}_{\varphi_j}^T \dot{\boldsymbol{\omega}}_{B/N} + c_{\varphi_j} \quad (67)$$

$$\ddot{\vartheta}_j = \mathbf{a}_{\vartheta_j}^T \ddot{\mathbf{r}}_{B/N} + \mathbf{b}_{\vartheta_j}^T \dot{\boldsymbol{\omega}}_{B/N} + c_{\vartheta_j} \quad (68)$$

ENERGY AND MOMENTUM DEFINITIONS

The total rotational kinetic energy (i.e. kinetic energy about the center of mass) of the spacecraft is:

$$T_{rot} = \frac{1}{2} \boldsymbol{\omega}_{\mathcal{B}/\mathcal{N}}^T [I_{bus, B_c}] \boldsymbol{\omega}_{\mathcal{B}/\mathcal{N}} + \frac{1}{2} m_{bus} \dot{\mathbf{r}}_{B_c, C} \cdot \dot{\mathbf{r}}_{B_c, C} + \sum_{j=1}^{N_P} \frac{1}{2} m_j \dot{\mathbf{r}}_{P_{c,j}/C} \cdot \dot{\mathbf{r}}_{P_{c,j}/C} \quad (69)$$

Expanding these terms and performing some simplification, Eq. (69) yields:

$$T_{rot} = \frac{1}{2} \boldsymbol{\omega}_{\mathcal{B}/\mathcal{N}}^T [I_{bus, B_c}] \boldsymbol{\omega}_{\mathcal{B}/\mathcal{N}} + \frac{1}{2} m_{bus} \dot{\mathbf{r}}_{B_c, B} \cdot \dot{\mathbf{r}}_{B_c, B} + \sum_{j=1}^{N_P} \frac{1}{2} m_j \dot{\mathbf{r}}_{P_{c,j}/B} \cdot \dot{\mathbf{r}}_{P_{c,j}/B} - \frac{1}{2} m_{SC} \dot{\mathbf{c}} \cdot \dot{\mathbf{c}} \quad (70)$$

The total rotational angular momentum of the spacecraft about point C is:

$$\mathbf{H}_{rot, C} = [I_{bus, B_c}] \boldsymbol{\omega}_{\mathcal{B}/\mathcal{N}} + m_{bus} \mathbf{r}_{B_c, C} \times \dot{\mathbf{r}}_{B_c, C} + \sum_{j=1}^{N_P} m_j \mathbf{r}_{P_{c,j}/C} \times \dot{\mathbf{r}}_{P_{c,j}/C} \quad (71)$$

Expanding Eq. (71) and rearranging the terms, the total rotation angular momentum is in the form:

$$\mathbf{H}_{rot, C} = [I_{bus, B_c}] \boldsymbol{\omega}_{\mathcal{B}/\mathcal{N}} + m_{bus} \mathbf{r}_{B_c, B} \times \dot{\mathbf{r}}_{B_c, B} + \sum_{j=1}^{N_P} m_j \mathbf{r}_{P_{c,j}/B} \times \dot{\mathbf{r}}_{P_{c,j}/B} - m_{SC} \mathbf{c} \times \dot{\mathbf{c}} \quad (72)$$

REFERENCE SYSTEM CHANGE

Seen in Eqs. (46), (47) and (48), the problem is singular for $\vartheta = \pi/2 + k\pi$, ($k = 0, 1, 2, \dots$). In order to solve this issue, a rotation of the pendulum frame, $\mathcal{P}_{0,j}$, is necessary. This rotation is performed when ϑ_j reaches a value multiple of $\pi/4$, to remain always far enough from the singularity. The new pendulum frame $\mathcal{P}_{0,j}^{new}$ is obtained with a rotation of the actual value of φ around the $\hat{\mathbf{p}}_{3,j}$ axis, and of ϑ around $\hat{\mathbf{p}}_{2,j}$ axis. This would lead to a new pendulum reference frame with $\hat{\mathbf{p}}_{1,j}^{new}$ aligned along the pendulum direction. The Fig. 4 shows the $\mathcal{P}_{0,j}^{new}$ respect to $\mathcal{P}_{0,j}$.

At this point is easy to see that the new value of φ_j and ϑ_j are equal to 0. To compute the new value of $\dot{\varphi}_j$ and $\dot{\vartheta}_j$, remembering the relation expressed in Eq. (32), Eq. (7) is reversed and it yields:

$$\dot{\varphi} = \frac{l'_j[2]}{l_j} \quad (73)$$

$$\dot{\vartheta} = -\frac{l'_j[3]}{l_j} \quad (74)$$

The integration can continue using these new values and the new reference systems. This would lead to discontinuities on φ_j , θ_j , φ_j and ϑ_j but not on the vectors l_j and l'_j .

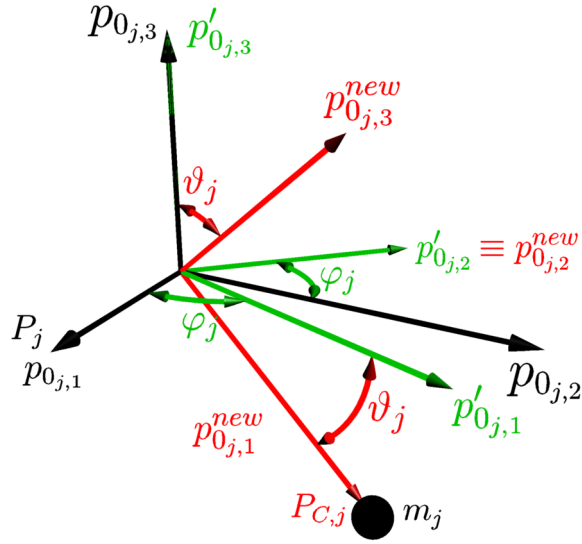


Figure 4: $\mathcal{P}_{0,j}^{\text{new}}$ frame definition

Table 1: GPS satellite data used in the simulated scenario

Launch mass	Dry mass	Size
3900 kg	2270 kg	3.4x2.5x1.8 m

SIMULATION AND VERIFICATION

To validate and test the code a simulation of the propellant slosh model has been run in the Basilisk software package. To reproduce a realistic situation, the case of a classical GPS satellite is considered here. The main parameters of the spacecraft and of the orbit are summarized in Table 1.

The orbit of the GPS satellite has been considered with an inclination of 55° , a semi-major axis of 26560.6 km, eccentricity of 0.02 an argument of perigee of 90° , and a right ascension of ascending node of 10° . At the beginning the propellant is considered at rest in the tank while the spacecraft suddenly the spacecraft rotates with an angular velocity of 0.01 rad/s around the x-axis. The motion of the hub induces a motion of the propellant in the tanks which starts to oscillate. This situation is simulated imposing the following design parameters:

$$\begin{aligned}
 l_1 = 0.3 \text{ m}, \quad m_1 = 500 \text{ kg}, \quad \dot{\varphi}_{1,0} = 0 \text{ rad/s}, \quad \dot{\vartheta}_{1,0} = 0 \text{ rad/s} \\
 \mathbf{d}_1 = \begin{bmatrix} 0.1 \\ 0.1 \\ 0.1 \end{bmatrix} m \quad \hat{\mathbf{p}}_{0,1} = \begin{bmatrix} \sqrt{2}/2 \\ 0 \\ \sqrt{2}/2 \end{bmatrix} \quad \hat{\mathbf{p}}_{0,2} = \begin{bmatrix} 0 \\ 1 \\ 0 \end{bmatrix} \quad \hat{\mathbf{p}}_{0,3} = \begin{bmatrix} -\sqrt{2}/2 \\ 0 \\ \sqrt{2}/2 \end{bmatrix} \quad (75)
 \end{aligned}$$

The following figures show how without a damping term the rotational and orbital angular momentum and energy are conserved. This is an important results that gives confidence in the correct derivation and implementation of the model. It has also been shown, without providing graphs here, that with reducing the time step the conservation quantities result in a higher accuracy. This gives further confidence that the model is correct because it confirms integration error is the only source of error.

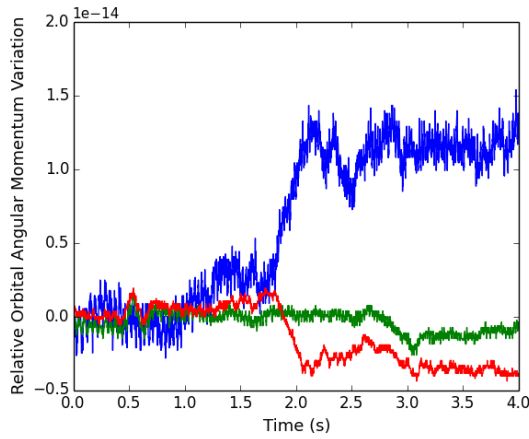


Figure 5: Relative Orbital Angular Momentum Variation

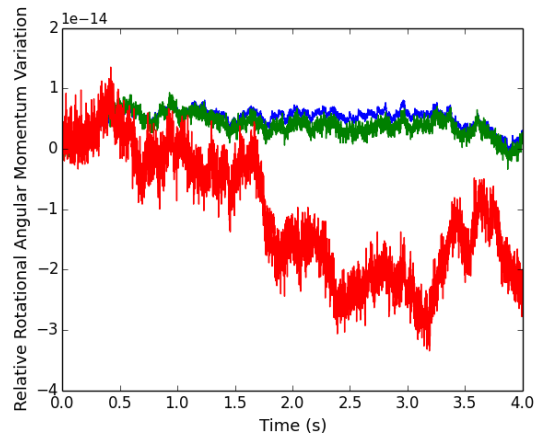


Figure 6: Relative Rotational Angular Momentum Variation

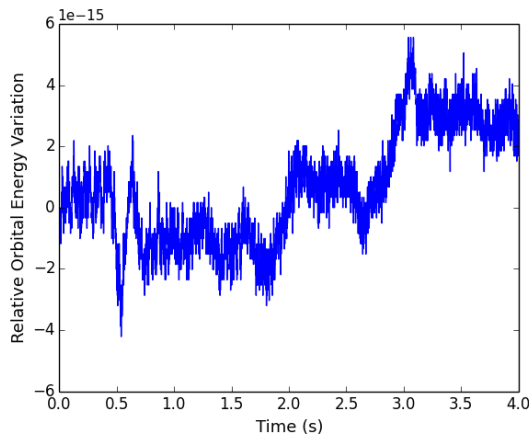


Figure 7: Relative Orbital Energy Variation

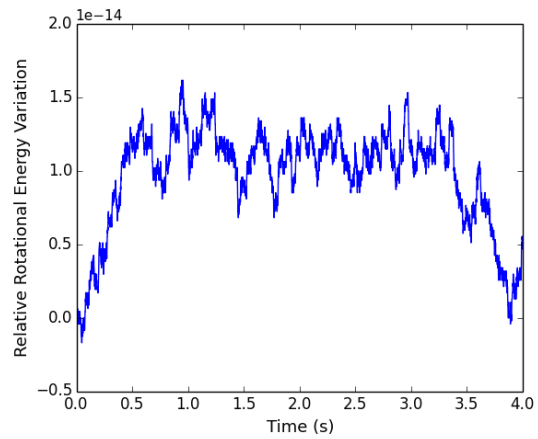


Figure 8: Relative Rotational Energy Variation

CONCLUSION

The fully-coupled equations of motion of a spacecraft with spherical pendulum based propellant slosh are derived. This formulation constitutes a mechanical approximation of a complex phenomenon. The advantage of this formulation is the possibility of fast and real time predictions of the sloshing phenomenon. The only way to predict the propellant motion with high accuracy is a CFD simulation but in most cases this is not applicable to long duration simulations of spacecraft.

Fuel slosh is of crucial importance for the design of the spacecraft control system. For this reason this mechanical model has been implemented in the Basilisk astrodynamics software package. This permits readily simulating a complex dynamics taking into account the propellant slosh effect on the dynamic of the spacecraft. The model has been verified by using the energy and momentum conservation applied to a GPS satellite.

Future developments of this work could involve an analysis of the limits of this model together with the analysis of a more complex mechanical model, considering both spherical pendulum and lumped spring mass model. Another feature could be considered for the Basilisk software package

is to provide an automatic method to set the design parameters starting from the tank and propellant properties. The final step to verify the robustness of this method is to compare it with CFD simulation of the same simulation setup.

ACKNOWLEDGMENTS

We wish to thank all the colleagues of the Autonomous Vehicle Systems (AVS) laboratory of University of Colorado Boulder for all the technical support. This work was funded in part by the ASI-CAIF grant.

REFERENCES

- [1] R. Lagier, "Ariane 5 User's Manual," Tech. Rep. Issue 5, Revision 2, Oct. 2016.
- [2] H. N. Abramson, "Representation of Fuel Sloshing in Cylindrical Tanks by an Equivalent Mechanical Model," *ARS Journal*, Vol. 31, Dec. 1961, pp. 1697–1705, 10.2514/8.5896.
- [3] V. Singal, J. Bajaj, N. Awalgaonkar, and S. Tibdewal, "CFD Analysis of a Kerosene Fuel Tank to Reduce Liquid Sloshing," *Procedia Engineering*, Vol. 69, 2014, pp. 1365–1371.
- [4] J. Hall, T. Rendall, C. Allen, and H. Peel, "A multi-physics computational model of fuel sloshing effects on aeroelastic behaviour," *Journal of Fluids and Structures*, Vol. 56, 2015, pp. 11–32.
- [5] B. Marsell, S. Gangadharan, Y. Chatman, J. Sudermann, K. Schlee, and J. Ristow, "A CFD Approach to Modeling Spacecraft Fuel Slosh," *Aerospace Sciences Meetings*, pp. –, American Institute of Aeronautics and Astronautics, Jan. 2009, 10.2514/6.2009-366.
- [6] M. Zucrow and J. Hoffman, *Gas dynamics*. No. v. 1 in Gas Dynamics, Wiley, 1976.
- [7] T. Schmitt, Y. Méry, M. Boileau, and S. Candel, "Large-Eddy Simulation of oxygen/methane flames under transcritical conditions," *Proceedings of the Combustion Institute*, Vol. 33, No. 1, 2011, pp. 1383 – 1390, <https://doi.org/10.1016/j.proci.2010.07.036>.
- [8] Y. Chatman, S. Gangadharan, K. Schlee, J. Ristow, J. Sudermann, C. Walker, and C. Hubert, "Modeling and Parameter Estimation of Spacecraft Fuel Slosh with Diaphragms Using Pendulum Analogs," *30th Annual American Astronautical Society (AAS) Guidance and Control Conference*, pp. –, American Astronautical Society, Feb. 2007.
- [9] F. Dodge, *The New "dynamic Behavior of Liquids in Moving Containers"*. Southwest Research Inst., 2000.
- [10] C. Allard, M. Diaz-Ramos, P. W. Kenneally, H. Schaub, and S. Piggott, "Modular Software Architecture for Fully-Coupled Spacecraft Simulations," *AAS Guidance and Control Conference*, Breckenridge, CO, Feb. 1–7 2018. Paper AAS 18-091.
- [11] J. Alcorn, C. Allard, and H. Schaub, "Fully Coupled Reaction Wheel Static and Dynamic Imbalance for Spacecraft Jitter Modeling," *Journal of Guidance, Control, and Dynamics*, 2018/04/02 2018, pp. 1–9, 10.2514/1.G003277.
- [12] C. J. Allard, M. Diaz Ramos, H. Schaub, and S. Piggott, "Spacecraft Dynamics Integrating Hinged Solar Panels and Lumped-Mass Fuel Slosh Model," *AIAA SPACE Forum*, pp. –, American Institute of Aeronautics and Astronautics, Sept. 2016, 10.2514/6.2016-5684.
- [13] C. Allard, H. Schaub, and S. Piggott, "General Hinged Solar Panel Dynamics Approximating First-Order Spacecraft Flexing," *AAS Guidance and Control Conference*, Breckenridge, CO, Feb. 5–10 2016. Paper No. AAS-16-156.
- [14] H. Schaub and J. L. Junkins, *Analytical Mechanics of Space Systems*. Reston, VA: AIAA Education Series, 3rd ed., 2014, 10.2514/4.102400.
- [15] G. H. Hardy and E. M. Wright, *An Introduction to the Theory of Numbers*. Mathematics, Oxford University press, 6th ed., 2008.
- [16] *Linear Least Squares Computations*. Statistics: A Series of Textbooks and Monographs, Taylor & Francis, 1988.